The EMBO Journal Vol.18 No.5 pp.1172–1181, 1999

Telomere shortening in mTR$^{-/-}$ embryos is associated with failure to close the neural tube

Eloísa Herrera, Enrique Samper and María A.Blasco[1]

Department of Immunology and Oncology, Centro Nacional de Biotecnología, CSIC, Campus de Cantoblanco, Madrid E-28049, Spain

[1]Corresponding author
e-mail: mblasco@cnb.uam.es

Mice genetically deficient for the telomerase RNA (mTR) can be propagated for only a limited number of generations. In particular, mTR$^{-/-}$ mice of a mixed C57BL6/129Sv genetic background are infertile at the sixth generation and show serious hematopoietic defects. Here, we show that a percentage of mTR$^{-/-}$ embryos do not develop normally and fail to close the neural tube, preferentially at the forebrain and midbrain. The penetrance of this defect increases with the generation number, with 30% of the mTR$^{-/-}$ embryos from the fifth generation showing the phenotype. Moreover, mTR$^{-/-}$ kindreds in a pure C57BL6 background are only viable up to the fourth generation and also show defects in the closing of the neural tube. Cells derived from mTR$^{-/-}$ embryos that fail to close the neural tube have significantly shorter telomeres and decreased viability than their mTR$^{-/-}$ littermates with a closed neural tube, suggesting that the neural tube defect is a consequence of the loss of telomere function. The fact that the main defect detected in mTR$^{-/-}$ embryos is in the closing of the neural tube, suggests that this developmental process is among the most sensitive to telomere loss and chromosomal instability.

Keywords: knock-out mouse/neural tube/telomerase/telomeres

Introduction

Neural tube defects, including spina bifida, anencephaly and congenital hydrocephalus, are among the major causes of infant mortality. The closing of the neural tube involves cell migration, proliferation and apoptosis. Although many genetic loci have been shown to be important in this complex developmental process (reviewed in Harris and Juriloff, 1997), the underlying molecular events that contribute to the neural tube closure are not yet well defined, and only a few genes have been shown to be involved (Epstein *et al*., 1991; Tassabehji *et al*., 1992; Imamoto and Soriano, 1993; Sah *et al*., 1995). Mouse models of neural tube defects are essential to unravel the molecular basis of this process. Here we show that mice null for the mouse telomerase RNA (mTR), an essential component of the telomerase reverse transcriptase complex, show defects in neural tube closure that are associated with telomere loss, increased chromosomal instability and loss of cell viability.

Telomerase is a reverse transcriptase that synthesizes telomeric repeats onto the ends of chromosomes (reviewed in Greider, 1996; Nugent and Lundblad, 1998). In vertebrates, telomeres consist of tandem repeats of the sequence TTAGGG (reviewed in Blackburn, 1991). In yeast, elimination of a telomere from a chromosome causes a RAD9-mediated cell-cycle arrest and loss of the chromosome (Sandell and Zakian, 1993). In mammals and yeast, telomere shortening to a critical length is associated with genetic instability and loss of cell viability (Counter *et al*., 1992; Singer and Gottschling, 1994; McEachern and Blackburn, 1995; Blasco *et al*., 1997; Lee *et al*., 1998; Naito *et al*., 1998; Nakamura *et al*., 1998; Niida *et al*., 1998).

Telomerase is composed of a catalytic protein subunit known as TERT (Harrington *et al*., 1997a; Kilian *et al*., 1997; Lingner *et al*., 1997; Meyerson *et al*., 1997; Nakamura *et al*., 1997; Greenberg *et al*., 1998; Martín-Rivera *et al*., 1998), an RNA molecule, or TR, that is used as template for the addition of new telomeric repeats (Greider and Blackburn, 1989; Singer and Gottschling, 1994; Blasco *et al*., 1995; Feng *et al*., 1995; McEachern and Blackburn, 1995), and a number of associated proteins (Collins *et al*., 1995; Harrington *et al*., 1997b; Nakayama *et al*., 1997; Gandhi and Collins, 1998).

Telomerase activity is present in cell types of unlimited life span, such as tumor cells and cells of the germ line (Autexier and Greider, 1996; Shay and Bacchetti, 1997), suggesting that telomere maintenance by telomerase is crucial in sustaining the growth of these cells. Indeed, the introduction of the telomerase catalytic subunit into primary non-immortal human cells that have no detectable telomerase activity is sufficient to restore enzymatic activity, to elongate and maintain telomeres and, in some cases, to allow immortal growth (Bodnar *et al*., 1998; Kiyono *et al*., 1998; Wang *et al*., 1998).

Telomerase is active during human embryonic development and it is down-regulated immediately after birth (Wright *et al*., 1997). Interestingly, the highest levels of human telomerase RNA (hTR) in human embryos are detected at the central nervous system (CNS), in particular in the primitive neuroepithelial cells of the neural tube surrounding the neural canal (Yashima *et al*., 1998). Differentiation of these cells is accompanied by down-regulation of hTR expression. Similarly, in the mouse, the two essential components of mouse telomerase, mTR and mTERT, are down-regulated after birth (Blasco *et al*., 1995; Greenberg *et al*., 1998). These observations suggest that telomere maintenance by telomerase may play a role in embryonic development.

The generation and characterization of a mouse strain null for the telomerase RNA, mTR$^{-/-}$, and therefore lacking

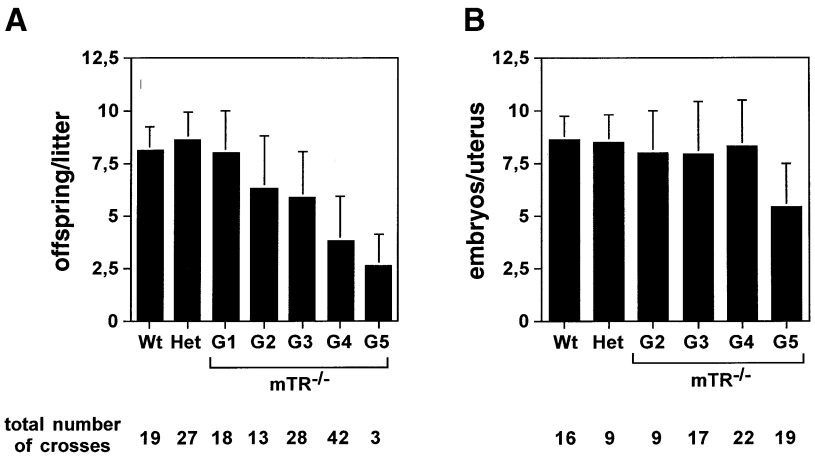

Fig. 1. Comparison of litter size of mTR$^{-/-}$ newborns versus *in utero* E10.5 mTR$^{-/-}$ embryos. (**A**) The average progeny per litter from wild-type, heterozygote or mTR$^{-/-}$ crosses from different generations is shown with bars. The total number of crosses of each genotype used for the analysis is indicated at the bottom of the graph. Wt, wild-type; Het, heterozygote. G1–G5 indicate the different generations of the mTR$^{-/-}$ newborns. Error bars are shown. (**B**) The average number of 10.5 day embryos found in the uterus of wild-type, heterozygote or different generation mTR$^{-/-}$ females is indicated with bars. Wt, wild-type; Het, heterozygote. G2–G5 indicate the different generations of the mTR$^{-/-}$ embryos. Standard deviation bars are shown.

telomerase activity, have been crucial in determining the role of telomerase in telomere maintenance, fertility and cell proliferation (Blasco *et al*., 1997; Lee *et al*., 1998). Telomerase activity is not required for the viability of mTR$^{-/-}$ mice during the first generations. However, telomeres shorten progressively and this shortening is accompanied by an increase in chromosomal abnormalities (Blasco *et al*., 1997; Hande *et al*., 1999b). In later generations, highly proliferative tissues such as those of the immune system, hematopoietic system and the germ line show defects in their proliferative capacity (Blasco *et al*., 1997; Lee *et al*., 1998). Here, we show that telomere loss in mTR$^{-/-}$ mice is associated with a developmental defect that consists of a failure to close the neural tube. These results suggest that telomeres have an important role during the formation of the neural tube. Moreover, cells derived from defective mTR$^{-/-}$ embryos show an increased apoptosis and a decreased viability. These observations support the idea that telomere maintenance above a threshold length is essential for cell viability in the context of the organism.

Results and discussion

Viability of mTR$^{-/-}$ embryos

mTR$^{-/-}$ mice of late generations show a marked decrease in litter size, which has been attributed to both male and female infertility (Lee *et al*., 1998; this study), but the occurrence of defects during embryonic development in late generation mTR$^{-/-}$ mice has remained unexplored. To distinguish parental infertility from embryonic lethality, we determined the number of 10.5 day embryos per uterus of pregnant mTR$^{-/-}$ females as a function of the generation number. The average litter size of wild-type, heterozygote and mTR$^{-/-}$ crosses is shown in Figure 1 as a function of the generation number; Figure 1A corresponds to the litter size of mice that are born and survived, whereas Figure 1B shows the number of 10.5-day-old embryos found in the uterus. The figure shows that the decrease in litter size is more pronounced than the decrease in the number of 10.5 day embryos. These results show that a fraction of 10.5 day mTR$^{-/-}$ embryos either do not survive gestation to completion or die immediately after birth, suggesting a developmental problem in a subset of embryos.

Analysis of wild-type and mTR$^{-/-}$ 10.5 day embryos

To address the role of telomerase in normal mouse development, we analyzed an average of 150 embryos of 10.5 days each from wild-type, heterozygote and mTR$^{-/-}$ crosses from different generations. A subset of mTR$^{-/-}$ embryos showed defects in neural tube closure (neural tube defects, NTDs; Table IA), whereas the progeny of wild-type crosses rarely showed such defects (Table IA). Remarkably, the percentage of mTR$^{-/-}$ embryos with NTD dramatically increased in the late generations, with 30% of the fifth generation embryos failing to close the neural tube by day 10.5 (see Table IA). To rule out the possibility that this embryonic defect was a consequence of inbreeding when deriving the different generations of mTR$^{-/-}$ mice (Blasco *et al*., 1997; Lee *et al*., 1998), we also analyzed mTR$^{-/-}$ mouse embryos that were 95% backcrossed to the C57BL/6J strain. Table IB shows that 15.2% of second generation mTR$^{-/-}$ 10.5 day embryos backcrossed on C57BL/6J also had an opened neural tube. The analysis of further generations of mTR$^{-/-}$embryos in the C57BL/6J background was not possible due to the fact that C57BL/6J mTR$^{-/-}$ mice are only fertile for the first four generations (E.Herrera and M.A.Blasco, unpublished results), in agreement with the fact that the C57BL/6J background has shorter telomeres than the mixed C57BL6/129sv background (see Table III; Hande *et al*., 1998).

Neural tube closure defects were observed at four different points in the nervous system: forebrain, midbrain (mesencephalon), cervical and caudal region (see examples in Figure 2A and B). Figure 2C shows histological sections of two mTR$^{-/-}$ embryos with the neural tube opened at the forebrain (panels a and b) or midbrain and tail (panels d and e). It is noticeable that some embryos with NTD had additional defects that affected the bilateral symmetry of the brain (see embryo in panels d and e), while most of the embryos with NTD had normal symmetry.

We quantified the frequency of NTD in the different

Table I. Failure to close the neural tube in $mTR^{-/-}$ 10.5 day embryos from different generations

Genotype	Generation	Total crosses	Embryos analyzed	No. of embryos with NTD	Incidence of NTD (%)
A. Embryos on a mixed C57BL/6J, 129Sv genetic background					
Wild-type	–	15	127	3	2.3
$mTR^{-/-}$	G3	21	155	14	9.0
$mTR^{-/-}$	G4	23	189	25	13.2
$mTR^{-/-}$	G5	19	123	37	30
B. Embryos on a C57BL/6J genetic background					
Wild-type	–	3	32	0	0
$mTR^{-/-}$	G2	6	46	7	15.2

areas of the nervous system (see Table II). More than 47% of the $mTR^{-/-}$ embryos with NTD had the opening in the midbrain area or mesencephalon and 40% in the forebrain (see Table II), while the rest of the embryos showed the opening in the cervical (7.8%) or the caudal (5.6%) areas (see Figure 2A and B for examples). The four areas in which closure defects were found coincide with the four sites at which the neural tube finally fuses (Sakai, 1989). In summary, we observe a defect in neural tube closure in embryos that lack mouse telomerase RNA and that are telomerase-deficient. We did not detect any other developmental defect in the $mTR^{-/-}$ embryos (except for the absence of bilateral symmetry in the brain in some embryos with NTD), suggesting that the neural tube formation is among the processes most sensitive to lack of telomerase during development. Interestingly, a subset of $p53^{-/-}$ mouse embryos also exhibit a neural tube closure defect preferentially in the midbrain; moreover, these $p53^{-/-}$ embryos also lacked bilateral symmetry in the brain (Sah *et al*., 1995).

mTR expression in mouse embryos

Previous studies have shown that mTR is expressed abundantly in the newborn brain and that this expression is down-regulated during the first 2 weeks after birth (Blasco *et al*., 1995). To study the expression of mTR during mouse embryonic development, we have performed whole-mount *in situ* hybridizations using a digoxigenin-labeled mTR probe (Figure 3). As a control, a 10.5 day $mTR^{-/-}$ embryo was hybridized with the antisense probe, showing no detectable expression of mTR, as expected from the fact that $mTR^{-/-}$ mice are null for the mTR gene (see Figure 3a). Similarly, 8.5-day (Figure 3b) and 10.5-day (Figure 3c) wild-type embryos were not stained by a sense probe except for a low background signal. Hybridization of wild-type 8.5 day embryos with the antisense probe revealed that mTR was expressed abundantly in the neural folds that will give rise to the future neural tube (Figure 3d, see arrows). In 10.5 day embryos (Figure 3e and f), mTR was expressed abundantly in the forebrain, midbrain, cervical area, tail and limbs (see arrows), similar to the expression pattern described for the mTERT mRNA (Martín-Rivera *et al*., 1998). The expression pattern of mTR in the developing mouse brain is consistent with the high level of hTR expression present in the CNS of early human embryos (Yashima *et al*., 1998), and suggests a role for telomerase activity and telomere maintenance during the formation of the neural tube.

Analysis of telomere length in $mTR^{-/-}$ embryos

It has been reported previously that $mTR^{-/-}$ mouse telomeres shorten ~5 kb per mouse generation due to the lack of telomerase activity, and that this shortening coincides with an increase in end-to-end chromosomal fusions and aneuploidy (Blasco *et al*., 1997; Hande *et al*., 1999b). The correlation between frequency of $mTR^{-/-}$ embryos showing open neural tubes and mouse generation suggests that the neural tube defect in $mTR^{-/-}$ embryos may be a consequence of telomere shortening and telomere loss from chromosome ends. In this regard, some murine models that develop neural tube abnormalities bear abnormal chromosomes, such as the trisomy 12 and trisomy 14 strains, with NTD in 100 or 50% of the embryos, respectively (Putz and Morriss-Kay, 1981). To determine whether the failure to close the neural tube in $mTR^{-/-}$ embryos was a consequence of telomere shortening and telomere loss in those embryos, we measured telomere length both in $mTR^{-/-}$ embryos with an opened neural tube and in embryos from the same uterus with a normal neural tube. Telomere length was measured in primary cells (mouse embryo fibroblasts; MEFs) derived from 10.5 day wild-type and $mTR^{-/-}$ embryos using quantitative fluorescence hybridization (Q-FISH) (Materials and methods). The average length of p- and q-telomeres from third and fourth generation $mTR^{-/-}$ embryos is shorter than that of wild-type embryos (Table III), as previously reported (Blasco *et al*., 1997). $mTR^{-/-}$ embryos on two different genetic backgrounds (see Table III) with an open neural tube have significantly shorter telomeres than embryos from the same uterus that do not present the phenotype (i.e. compare 16.79 ± 11.46 kb for all telomeres in the NTD embryo KO-$G3^b$, with 46.9 ± 23.5 kb for the normal embryo, KO-$G3^a$). Most importantly, in all the embryos with the neural tube closure defect, we detected an increase in the number of chromosome ends that do not show detectable TTAGGG sequences as compared with littermates that do not show the phenotype (Table III). As shown in Table III, the number of ends lacking detectable telomeres correlates with the appearance of the NTD phenotype. Figure 4 shows representative images of metaphase chromosomes derived from a wild-type embryo (Figure 4a) and from two $mTR^{-/-}$ embryos from the same uterus, one with a normal neural tube (embryo KO-$G3^a$, Figure 4b) and one with a defect in neural tube closure (embryo KO-$G3^b$, Figure 4c). Figure 4 also shows metaphases derived from littermate $mTR^{-/-}$ embryos (from the same uterus) on the C57BL/6J background with a normal neural tube

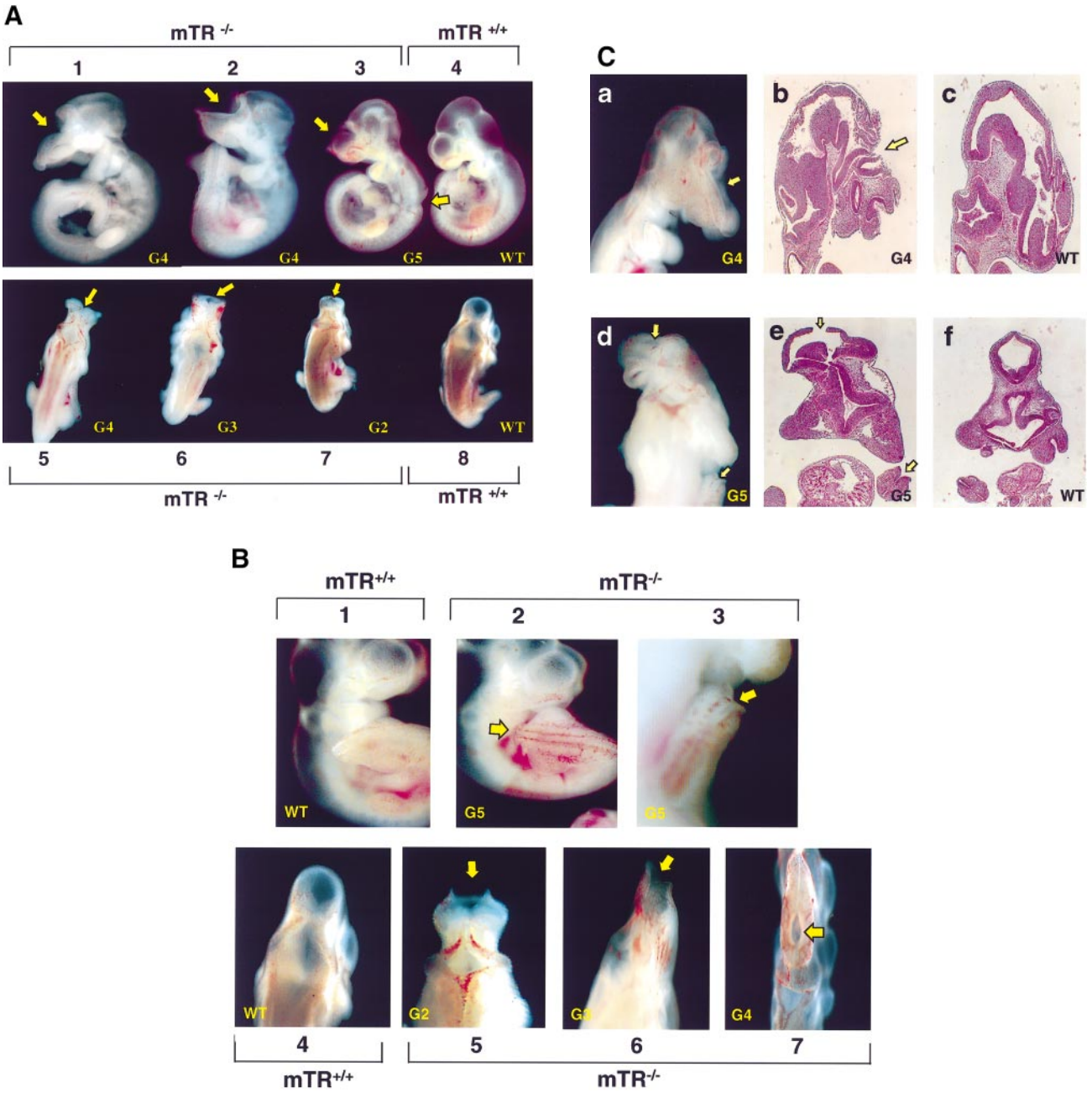

Fig. 2. Images of wild-type and mTR$^{-/-}$ 10.5 day embryos. (**A**) The upper part of the figure shows a lateral view of four 10.5 day mouse embryos. Embryo number 4 corresponds to a wild-type with a normal neural tube. Embryos 1, 2 and 3 are mTR$^{-/-}$ embryos from the indicated generations, all showing an opened neural tube at the level of the forebrain (see yellow arrows to localize openings). Embryo 3 also shows an opened neural tube at the level of the cervical area (see arrow). The lower part of the figure shows dorsal views of four 10.5 day mouse embryos. Embryo 8 is wild-type and shows a closed neural tube. Embryos 5, 6 and 7 show the neural tube open in the mesencephalon (see yellow arrows to localize the opening). G2–G5 correspond to second to fifth generation embryos, respectively. (**B**) Details of neural tube openings at different points of the nervous system. Embryos 1 and 4 are 10.5 day wild-type embryos with a normal neural tube. Embryos 2 and 3 show the neural tube open in the caudal area (see arrows). Embryos 4, 5 and 6 show the neural tube open at the mesencephalon. G2–G5 correspond to first to fifth generation embryos, respectively. (**C**) Histological analysis of 10.5 day wild-type and mTR$^{-/-}$ embryos. (a) and (d) Two different mTR$^{-/-}$ embryos with NTD; (b) and (e), the corresponding histological sections. (b) A sagittal section of the mTR$^{-/-}$ embryo shown in (a); the arrow points to the neural tube opening in the forebrain. (c) The equivalent sagittal section of a wild-type embryo. Notice the different structure of the mTR$^{-/-}$ brain. (e) A coronal section of the mTR$^{-/-}$ embryo shown in (d); the arrows point to the neural tube opening in the mesencephalon and the tail. (f) An equivalent section of a wild-type embryo. Notice that the bilateral symmetry of the mTR$^{-/-}$ embryo is altered. Wt, wild-type: G4 and G5, fourth and fifth generation, respectively.

(embryo KO-G3^{c}, Figure 4d) or with a neural tube closure defect (embryo KO-G3^{d}, Figure 4e). The telomeric signal in cells derived from NTD mTR$^{-/-}$ embryos on both genetic backgrounds was much lower than in cells derived from the corresponding normal littermate embryos (from the same uterus) (compare Figure 4c and e with b and d; Table III). Moreover, the mTR$^{-/-}$ embryos with the neural tube defect showed a larger number of chromosome ends with decreased telomeric signal (Figure 4, see yellow arrows; Table III), as well as an increase in chromosome

Table II. Localization of neural tube defects in mTR$^{-/-}$ 10.5 day embryos

Generation	Forebrain	Midbrain	Cervical area	Caudal area
G2	2	10	0	0
G3	3	6	0	2
G4	17	14	4	2
G5	13	12	3	1
Total No. of abnormal embryos	35	42	7	5
Percentage with respect to the total No. of defective neural tubes	40	47	7.8	5.6

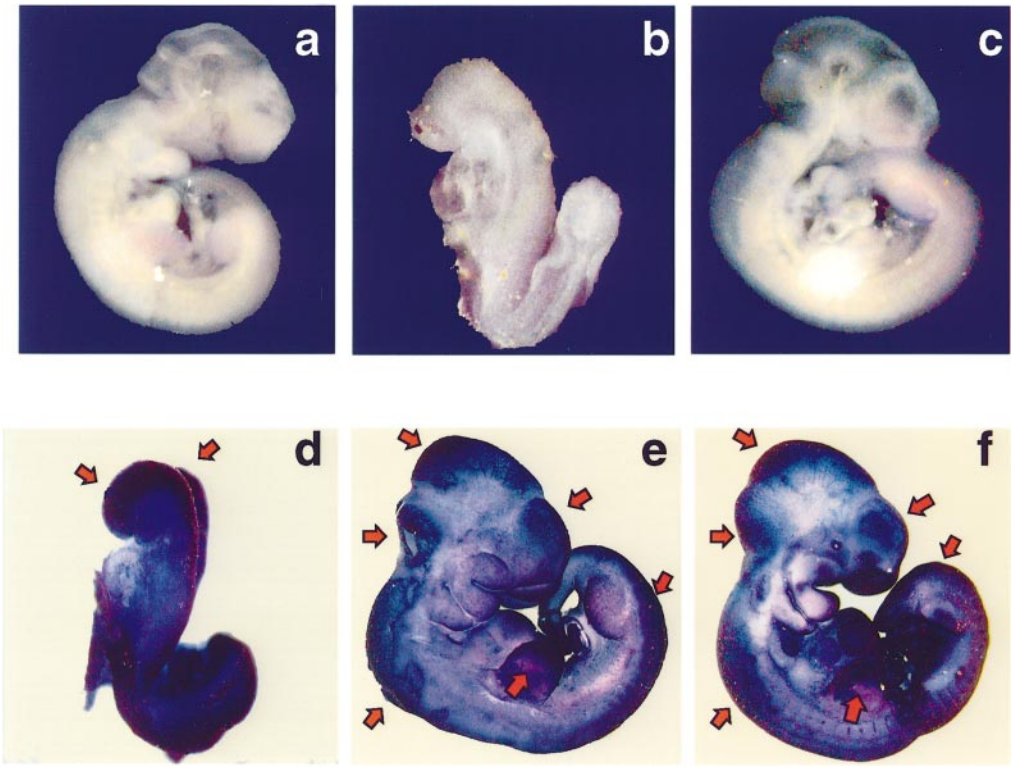

Fig. 3. Expression of mTR RNA in mouse embryos. (**a**) Eight and a half day mTR$^{-/-}$ embryo hybridized with an antisense mTR-derived riboprobe. Eight and a half day (**b**) and 10.5 day (**c**) wild-type embryos hybridized with sense mTR-derived riboprobes. Eight and a half day (**d**) and 10.5 day (**e** and **f**) wild-type embryos hybridized with antisense mTR-derived riboprobes. Regions of particularly high levels of mTR RNA are indicated with arrows.

Table III. Chromosomal abnormalities and telomere length in primary cells derived from wild-type and mTR$^{-/-}$ 10.5 day embryos with NTD

	Neural tube	Metaphases analyzed	End-to-end associations (frequency per metaphase)	Telomeres without detectable TTAGGG repeats/ total chromosomes[e]	TFUs of individual telomeres (mean ± SD)		
					All	p-arm	q-arm
Wild-type	closed	10	0	0/396 (0%)	54.17 ± 17.88	46.15 ± 16.5	61.89 ± 19.25
KO-G3[a]	closed	10	0	4/400 (4%)	46.9 ± 23.5	34.9 ± 20.1	58.9 ± 27.04
KO-G3[b]	open	10	0.2	63/379 (17%)	16.79 ±11.46	14.21 ± 10.5	19.38 ± 12.38
KO-G3[c] (C57BL/6J)	closed	10	0.1	12/398 (3%)	22.75 ± 15.60	17.95 ± 13.34	27.48 ± 17.86
KO-G3[d] (C57BL/6J)	open	10	0	75/400 (19%)	13.94 ± 9.93	13.32 ± 10.49	14.57 ± 9.36
KO-G4[a]	closed	10	0	14/388 (3.6%)	31.42 ± 23.46	25.52 ± 15.48	37.33 ± 20.46
KO-G4[b]	open	10	0.4	43/398 (11%)	27.46 ± 18.9	20.45 ± 16.0	35.08 ± 21.78

KO-G3[a] and KO-G3[b] are littermate mTR$^{-/-}$ embryos from the third generation.
KO-G3[c] and KO-G3[d] are littermate mTR$^{-/-}$ embryos from the third generation on the C57BL/6J genetic background.
KO-G4[a] and KO-G4[b] are littermate mTR$^{-/-}$ embryos from the third generation.
[e]We estimated that those ends lacking telomeric signal have <0.3 kb telomeric repeats.

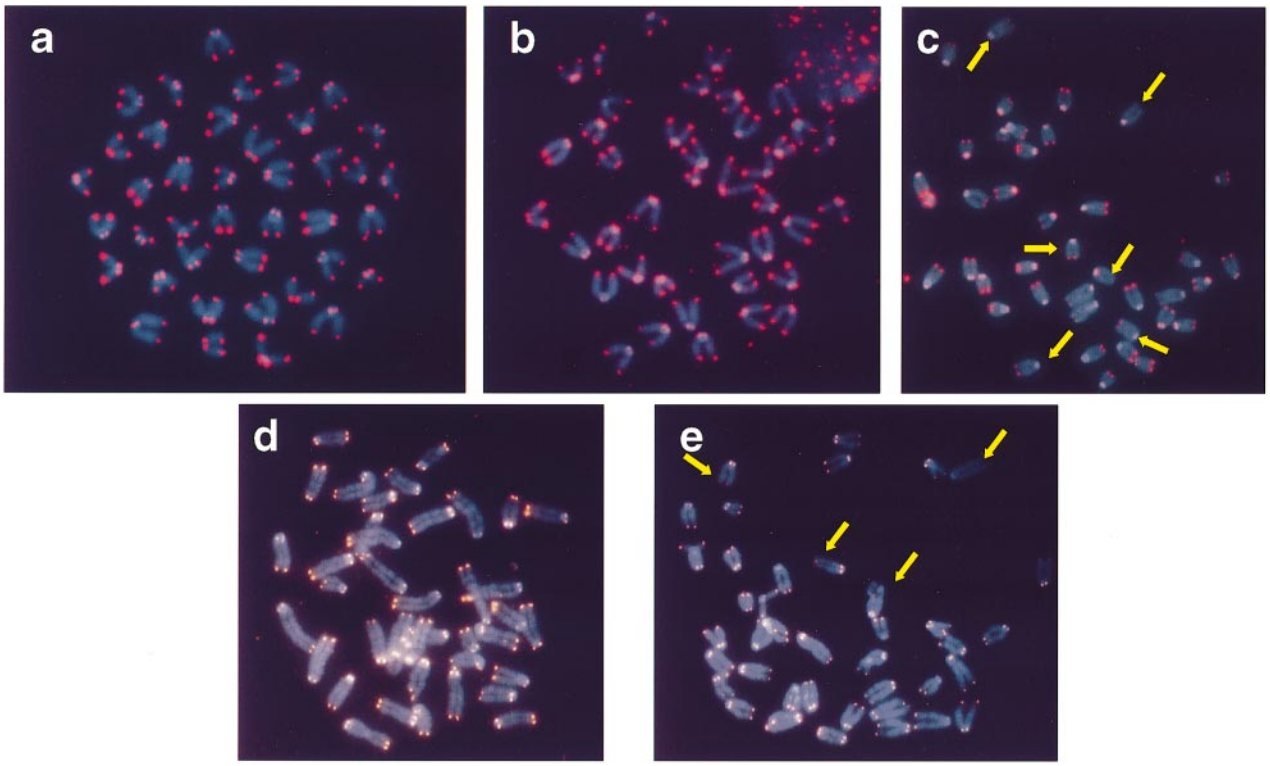

Fig. 4. Metaphases from wild-type and mTR$^{-/-}$ 10.5 day embryos of different generations. (a–c) Metaphases from third generation 10.5-day wild-type and third generation mTR$^{-/-}$ embryos. (**a**) A metaphase corresponding to wild-type cells; (**b**) a metaphase of cells derived from an mTR$^{-/-}$ embryo (KO-G3^{a} in Table III) with a normal neural tube; (**c**) metaphase chromosomes of cells derived from an mTR$^{-/-}$ embryo (KO-G3^{b} in Table III) from the same uterus with a defect in neural tube closure. Yellow arrows indicate the chromosome ends that lack detectable TTAGGG repeats. Quantification of telomere length of these cells is shown in Table III. (d and e) Metaphases from 10.5 day wild-type and third generation mTR$^{-/-}$ embryos 95% backcrossed to C57BL/6J. (**d**) A metaphase corresponding to cells derived from an mTR$^{-/-}$ embryo (KO-G3^{a} in Table III) with a normal neural tube; (**e**) a metaphase corresponding to cells derived from a littermate mTR$^{-/-}$ embryo (from the same uterus) (KO-G3^{b} in Table III) with the neural tube open. Yellow arrows indicate the chromosome ends lacking TTAGGG repeats. Quantification of telomere length is in Table III.

fusions (Table III). This association between a decreased telomeric signal and NTD strongly suggests that the neural tube closure defect may be a consequence of telomere shortening to a critical length. Furthermore, the fact that telomere length is very heterogeneous for a given chromosome among littermates (Ziljmans *et al*., 1997; Hande *et al*., 1999a; see Figure 4) could explain why the NTD is observed only in a subset of mTR$^{-/-}$ embryos in each generation, presumably in those embryos that had the shortest telomeres at critical chromosomes.

Decreased viability and increased apoptosis in mTR$^{-/-}$ embryos showing NTD

It has been described previously in yeast and in mice that telomere loss from critical chromosomes may affect cell viability (Sandell and Zakian, 1993; Lee *et al*., 1998). Indeed, several embryos with an open neural tube were in the process of being reabsorbed at day 10.5 (not shown).

To test whether the neural tube closure defect found in some mTR$^{-/-}$ embryos is accompanied by a decrease in the proportion of proliferating cells or, alternatively, by an increase in apoptotic cells, we have carried out *in situ* bromodeoxyuridine (BrdU) incorporation assays and whole-mount terminal deoxynucleotidyl transferase-mediated dUTP-biotin nick end labeling (TUNEL) assays. The *in situ* BrdU assays were carried out in wild-type and in mTR$^{-/-}$ embryos from different generations. Figure 5A shows a detail of a sagittal section of a 10.5 day wild-type embryo with abundant S-phase activity throughout the embryo and especially in the neural tube region, in agreement with the fact that this is an area of intense proliferation. Figure 5B corresponds to a similar section of a fifth generation 10.5 day mTR$^{-/-}$ embryo with an open neural tube at the forebrain and at the caudal area (arrows). No big differences were detected in the number of BrdU-positive nuclei in the NTD embryo with respect to the wild-type embryo with a normal neural tube (Figure 4b). However, we could not rule out that a specific population of cells important in neural tube formation are indeed arrested as a consequence of telomere loss. To ascertain whether apoptosis was increased in mTR$^{-/-}$ embryos from late generation, we used the TUNEL assay on whole-mount 8.5 day mTR$^{-/-}$ embryos (see Figure 6). We detected a higher apoptosis signal in the 8.5 day mTR$^{-/-}$ embryos (5–7) than in the wild-type counterparts (1–3). Figure 6 also shows a negative control where no TdT was added (embryo number 4). The fact that at day 8.5 (neural fold stage) there is more detectable apoptosis in mTR$^{-/-}$ embryos (i.e. embryo number 6) than in control wild-type embryos could explain, in part, the occurrence of NTD in a fraction of the 10.5 day mTR$^{-/-}$ embryos. Moreover, the high expression of mTR at the neural fold stage in wild-type embryos is consistent with a role for telomere maintenance in the development of the neural tube.

To quantify the differences in viability between mTR$^{-/-}$

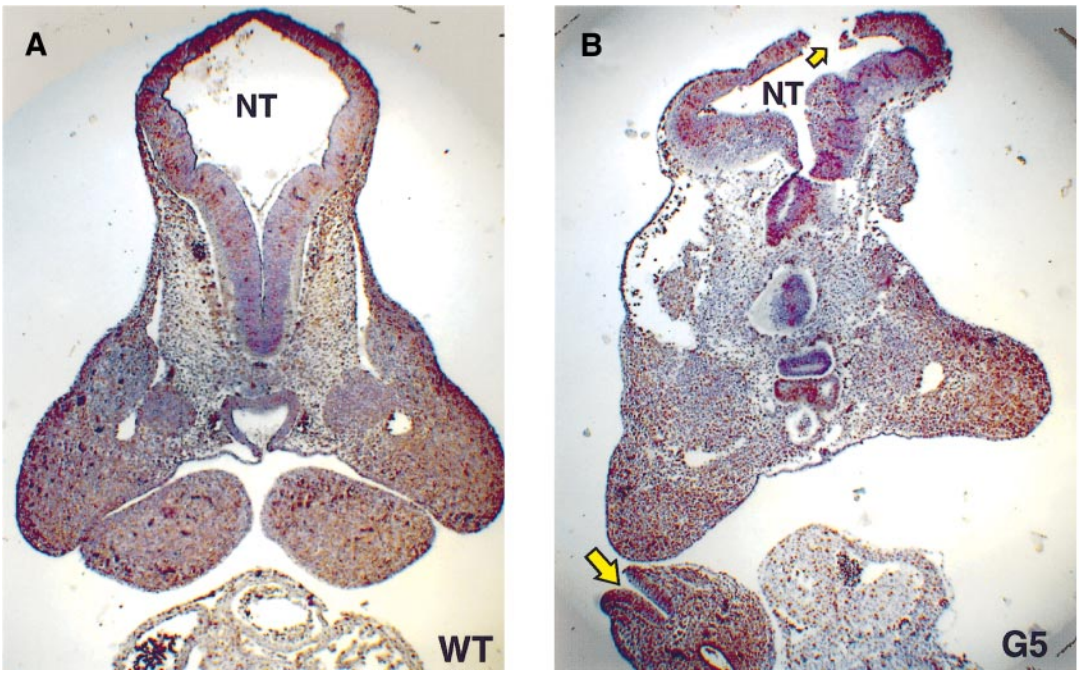

Fig. 5. *In situ* assays to measure BrdU incorporation in 10.5 day embryos and viability assays. (**A**) A detail from a sagittal section of a 10.5 day wild-type embryo after the BrdU incorporation *in situ* assay, showing BrdU-positive (black) nuclei in the whole section and particularly in the neural tube (NT). (**B**) Sagittal section of a fifth generation 10.5 day mTR$^{-/-}$ embryo (G5) with the neural tube open at two sites (see arrows indicating the openings in the midbrain and the caudal area). NT, neural tube.

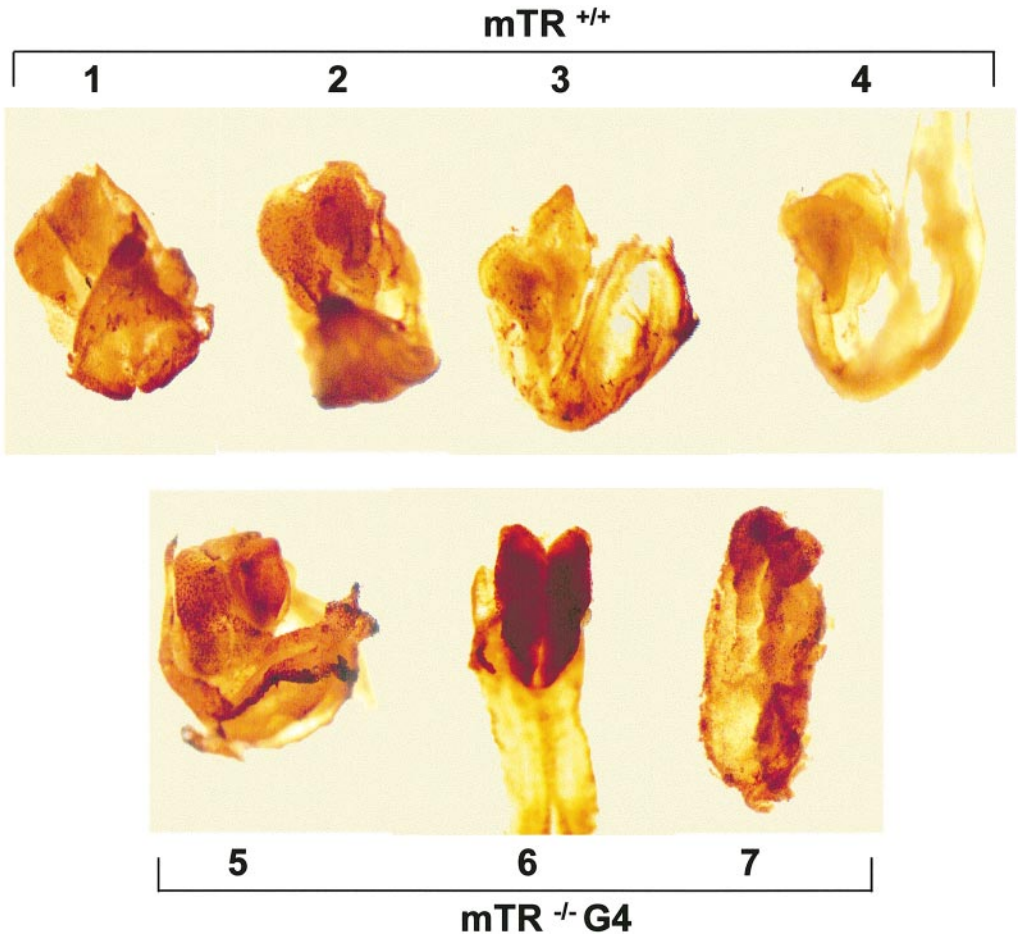

Fig. 6. Whole-mount TUNEL on 8.5 day embryos (neural fold stage). Embryos 1–3 are wild-type (mTR$^{+/+}$) and embryos 5–7 are mTR$^{-/-}$embryos from the fourth generation (G4). Embryo 4 was used as a negative control and no TdT was added when the TUNEL assay was performed. Apoptosis is detected as brown dots.

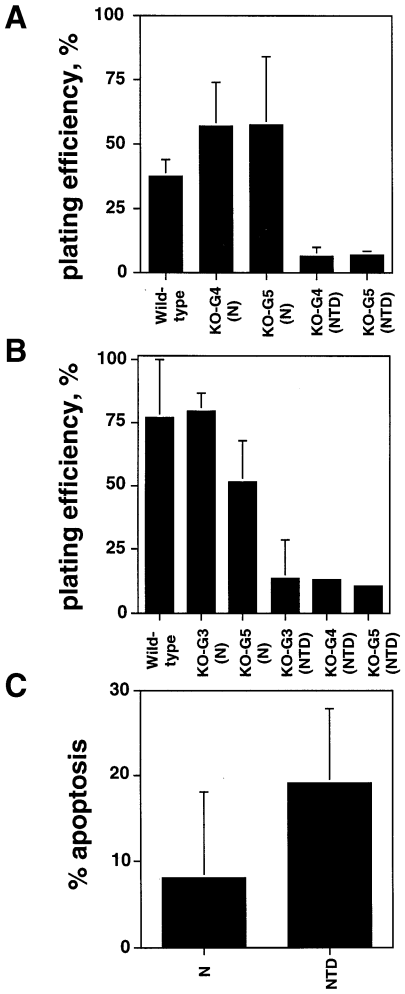

Fig. 7. Viability assays. (**A**) Plating efficiency of total cells derived from 10.5 day wild-type and mTR$^{-/-}$ embryos from a different generation showing NTD or a normal neural tube (N). KO-G4 and KO-G5, mTR$^{-/-}$ embryos from the fourth and fifth generation, respectively. N, normal; NTD, neural tube defect. The values are averages of three or more embryos. Error bars are shown. (**B**) Plating efficiency of MEFs derived from 10.5 day wild-type and several generation mTR$^{-/-}$ embryos showing NTD or a normal neural tube (N). KO-G3, KO-G4 and KO-G5 are third, fourth and fifth generation mTR$^{-/-}$ embryos, respectively. The values are averages of three or more embryos. Error bars are shown. (**C**) Percentage of apoptosis as measured by FACS analysis in total cells derived from mTR$^{-/-}$ embryos showing NTD or a normal neural tube (N). The values are the averages of three different embryos. Standard deviation bars are shown.

and wild-type embryos, we have compared the plating efficiency of total cells directly derived from control wild-type embryos and from normal or NTD mTR$^{-/-}$ embryos. We found that total cells derived from wild-type or mTR$^{-/-}$ embryos with a normal neural tube had a plating efficiency of ~50% (Figure 7A), whereas cells derived from mTR$^{-/-}$ embryos showing NTD had a very reduced plating efficiency (<10%) (Figure 7A). Similar results were obtained when we measured plating efficiency in MEFs derived from either wild-type or mTR$^{-/-}$ embryos (Figure 7B). Importantly, when we carried out a fluorescence-activated cell sorting (FACS) analysis of total cells derived from littermate mTR$^{-/-}$ embryos with a normal tube (N) or showing NTD (NTD) (Figure 7C), we found an increased apoptosis (~20%) in the cells derived from embryos that had the open neural tube as compared with that detected in those derived from littermates with a normal tube (~7%). These results indicate that cells derived from mTR$^{-/-}$ embryos showing NTD have a severe defect in viability, as measured both by a decreased plating efficiency and an increased apoptosis.

In summary, we have shown that telomere shortening and telomere loss in mTR$^{-/-}$ embryos is associated with a defect in the closing of the neural tube. Our observations suggest that the closing of the neural tube is among the most sensitive processes of the developing embryo to telomere loss and chromosomal instability, possibly due to the massive proliferation that occurs during early development for the formation of the CNS. The fact that mTR is highly expressed during the formation of the neural tube, together with the fact that the human homologue of mTR, hTR, is also expressed abundantly at the CNS in early human embryos (Yashima *et al*., 1998), implies an important role for telomere maintenance during the neural tube formation and explains the occurrence of the phenotype. It would be interesting to test if some cases of infant neural tube defects are associated with telomere shortening.

Materials and methods

Analysis of embryos

Wild-type, heterozygote and mTR$^{-/-}$ mice from different generations were mated. The day on which the vaginal plug was detected was considered to be day 0.5 post-coitum (p.c.). Pregnant females were sacrificed 8.5 and 10.5 days p.c. and the embryos removed for analysis. Images were captured using a Leica camera coupled to a dissecting scope, then transferred to the Adobe Photoshop program.

For histological analysis, 10.5 day embryos were fixed in formalin, dehydrated in ethanol, embedded in paraffin, sectioned (6 μm) and stained with Harris hematoxylin and eosin (Merck).

Other embryos were allocated for histology, TUNEL and BrdU *in situ* assays, or to derive MEFs, as described below.

Cell isolation from embryos

MEFs were derived from 10.5 day embryos as described (Blasco *et al*., 1997). At 24 h after plating in Dulbecco's modified Eagle's medium (DMEM) supplemented with 20% fetal bovine serum (FBS), MEFs were put in the presence of colcemid to be processed for Q-FISH analysis (see below). Alternatively, cells were allocated for viability assays or for FACS (see below).

Plating efficiency

To measure plating efficiency, either total cells or MEFs derived from wild-type and mTR$^{-/-}$ embryos were counted and 10 000 cells were plated in serum-supplemented DMEM. At 6 h after plating, cells were counted and the percentage of cells attached to the plate was calculated.

Whole mount in situ hybridization

A *Pst*I DNA fragment from mTR was cloned in pBluescript SK^{-}, digested at the 5′ or 3′ end of the insert and transcribed in the presence of digoxigenin (Riboprobe Kit, Promega) with T7 or T3 RNA polymerase, respectively. Mouse embryos were fixed in 4% paraformaldehyde at 4°C for 12 h. Embryos were treated with 6% hydrogen peroxide for clearing. Pre-hybridization was done at 70°C for 1 h in a solution containing 50% formamide, 5× SSC, 0.1 mg/ml yeast RNA, 1% SDS and heparin. After this, the probe was added to the pre-hybridization solution and incubation was continued at 70°C for 16 h. Embryos were washed and transferred to a blocking solution containing 1% Tween-20, 20% FBS and 1× blocking powder. The embryos were then incubated with anti-digoxigenin antibody (anti-digoxigenin-Ap Fab fragments) for 16 h at 4°C, and the signal developed using NBT/BCIP (Boehringer Mannheim). Images were captured using a Leica MZAPO and transferred to Adobe Photoshop 3.0.

Quantitative fluorescence in situ hybridization

Primary embryonic fibroblasts from 10.5 day mTR$^{+/+}$ (wild-type) and normal or NTD mTR$^{-/-}$ from several generations were harvested follow-

ing 4–5 h treatment with colcemid (0.1 μg/ml). Cells were trypsinized and centrifuged (120 *g*, 8 min). After hypotonic swelling in sodium citrate (0.03 M) for 25 min at 37°C, cells were fixed in methanol:acetic acid (3:1). After 2–3 additional fixative changes, the cell suspension was dropped on wet, clean slides and dried overnight. FISH was performed essentially as described (Zijlmans *et al*., 1997).

The Cy-3-labeled $(C_3TA_2)_3$ PNA probe (Perseptive Biosystems, Bedford, MA) was dissolved in a hybridization buffer containing 70% formamide, 10 mM Tris pH 7.0, 0.25% (w/v) blocking reagent (Boehringer Mannheim) at a concentration of 0.5 μg/ml. The hybridization mixture (2× 10 ml) was placed on the slides and a coverslip (22×60 mm) was applied followed by DNA denaturation (3 min, 80°C). After hybridization for 2 h at room temperature, slides were washed twice for 15 min each with 70% formamide, 10 mM Tris pH 7.2 and three times for 5 min each with 0.05 M Tris/0.15 M NaCl pH 7.5/0.05% Tween-20. Slides were dehydrated in an ethanol series and air-dried. Slides were counterstained with 4′,6-diamidino-2-phenylindole (DAPI) (0.2 μg/ml) in Vectashield (Vector Laboratories, Burlingame, CA).

Digital images were recorded with a COHU High Performance CCD camera model 49-12-5000 on a Leica Leitz DMRB fluorescence microscope (Leica, UK) equipped with a red fluorescence filter (Leica I3-513808) and a DAPI fluorescence filter (Leica A-513808) both located on a manual wheel. Images were acquired with the Q-FISH software package (Leica Imaging Systems, UK), using a 100×/NA 1.0 objective lens (Leica) and a 100 W mercury/xenon lamp (Leica). A dedicated computer program was used for image analysis as described (Zijlmans *et al*., 1997). The integrated fluorescence intensity for each telomere was calculated after correction for image acquisition exposure time. A minimum of 10 metaphases per group was analyzed.

Calibration

The details of calibration for telomere fluorescence intensity are explained elsewhere (Martens *et al*., 1998). Briefly, we used two levels of calibration to ensure a reliable quantitative estimate of telomere length in various samples. First, to correct for daily variations in lamp intensity and alignment, images of fluorescent beads were acquired and analyzed with the 'Image Analysis' computer program. Secondly, relative telomere fluorescence units (TFUs) were extrapolated from the plasmid calibration. For this, we hybridized and analyzed plasmids with a defined $(TTAGGG)_n$ length of 0.15, 0.40, 0.80 and 1.60 kb (Hanish *et al*., 1995). There was a linear correlation (r = 0.986) for plasmid fluorescence intensity and $(TTAGGG)_n$ length, with a slope of 47.7. The calibration-corrected telomere fluorescence intensity (ccTFI) of each telomere was calculated according to the formula: ccTFI = (Bea1/Bea2)×(TFI/47.7); where Bea1 = fluorescence intensity of beads when plasmids were analyzed, Bea2 = fluorescence intensity of beads when sample x was analyzed and TFI = unmodified fluorescence intensity of a telomere in sample x. Following this, the ccTFI of individual telomeres is expressed in TFUs, in which one unit corresponds to 1 kb of plasmid TTAGGG repeats.

In situ assays to measure BrdU incorporation

At 10.5 days p.c., wild-type and $mTR^{-/-}$ pregnant females received i.p. injections of BrdU [Boehringer Mannhein, 1 mg/g body weight in phosphate-buffered saline (PBS)]. The mice were sacrificed 1 h after the injection. Embryos were fixed, dehydrated with increasing ethanol concentrations, embedded in paraffin and sectioned (6 μm). The sections were dewaxed, hydrated and treated with 1% H_2O_2 in methanol to block endogenous peroxidase activity and with 2 M HCl for DNA denaturation. Sections were incubated with mouse monoclonal anti-BrdU antibody (Beckton-Dickinson) for 3 h followed by a biotinylated goat anti-mouse antibody (Amersham). The signal was amplified with the Vectastain ABC Kit (Vector Laboratories) and visualized with 3,3′-diaminobenzidine (DAB, Sigma); sections were counterstained with Harris hematoxylin stain (Sigma).

Whole-mount TUNEL assays

Wild-type and $mTR^{-/-}$ 8.5 day embryos (neural fold stage) were fixed with 4% paraformaldehyde–PBS and then transferred to 70% ethanol. Embryos were rehydrated and incubated in methanol:30% H_2O_2 (4:1) for 1 h. After three washes in PBT (PBS with 0.1% Tween-20), embryos were incubated for 5 min with proteinase K (15 μg/ml) followed by two incubations of 5 min each in glycine (2 mg/ml). Embryos were fixed again in 4% paraformaldehyde–0.2% glutaraldehyde–PBS for 1 h and then washed three times in PBT. The detection of apoptosis was carried out using the *in situ* Cell Detection Kit, POD (Boehringer Mannheim). The reactions were stopped with four washes of 30 min each in 300 mM Na citrate–0.1% Tween-20, and embryos were incubated for 1 h at room temperature in Converted-POD (Kit) previously pre-adsorbed in embryo powder and 0.1% fetal serum. After four washes in PBS, signal was developed with DAB (Sigma) and 0.3% H_2O_2 until visible staining was detected. Embryos were then washed in PBS and images were captured using a Leica MZAPO and transferred to Adobe Photoshop 3.0.

Acknowledgements

We are very grateful to Peter Lansdorp for providing the FISH analysis program, as well as for constant advice. We are indebted to Juan Martín-Caballero and Jessica Freire for their assistance in establishing the different mouse generations. We thank Manuel Serrano, Carol W.Greider, Carlos Martínez-A, Han Woong Lee, Cathy Mark and Miguel Torres for their helpful suggestions. E.H. is supported by a predoctoral fellowship from the Department of Immunology and Oncology. E.S. is supported by a predoctoral fellowship from The Regional Goverment of Madrid. Research at the laboratory of M.A.B. is funded by grants PM95-0014 and PM97-0133 from the Ministry of Education and Culture, Spain, by grant 08.1/0030/98 from The Regional Goverment of Madrid, and by the Department of Immunology and Oncology. The Department of Immunology and Oncology was founded and is supported by the Spanish Research Council (CSIC) and by Pharmacia and Upjohn.

References

Autexier,C. and Greider,C.W. (1996) Telomerase and cancer: revisiting the telomere hypothesis. *Trends Biochem*., **21**, 387–391.

Blackburn,E.H. (1991) Structure and function of telomeres. *Nature*, **350**, 569–573.

Blasco,M.A., Funk,W.D., Villeponteau,B. and Greider,C.W. (1995) Functional characterization and developmental regulation of mouse telomerase RNA. *Science*, **269**, 1267–1270.

Blasco,M.A., Lee,H.-W., Hande,P., Samper,E., Lansdorp,P., DePinho,R. and Greider,C.W. (1997) Telomere shortening and tumor formation by mouse cells lacking telomerase RNA. *Cell*, **91**, 25–34.

Bodnar,A.G. *et al*. (1998) Extension of life-span by introduction of telomerase into normal human cells. *Science*, **279**, 349–352.

Collins,K., Kobayashi,R. and Greider,C.W. (1995) Purification of *Tetrahymena* telomerase and cloning of the genes for the two protein components of the enzyme. *Cell*, **81**, 677–686.

Counter,C.M., Avilion,A.A., LeFeuvre,C.E., Stewart,N.G., Greider,C.W., Harley,C.B. and Bacchetti,S. (1992) Telomere shortening associated with chromosome instability is arrested in immortal cells which express telomerase activity. *EMBO J*., **11**, 1921–1929.

Epstein,D.J., Vekemans,M. and Gros,P. (1991) *splotch* (Sp<2H>), a mutation affecting development of the mouse neural tube, shows a deletion within the paired homeodomain of Pax-3. *Cell*, **67**, 767–774.

Feng,J. *et al*. (1995) The RNA component of human telomerase. *Science*, **269**, 1236–1241.

Gandhi,L. and Collins,K. (1998) Interaction of recombinant *Tetrahymena* telomerase proteins p80 and p95 with telomerase RNA and telomeric DNA substrates. *Genes Dev*., **12**, 721–733.

Greenberg,R.A., Allsopp,R.C., Chin,L., Morin,G. and DePinho,R. (1998) Expression of mouse telomerase reverse transcriptase during development, differentiation and proliferation. *Oncogene*, **16**, 1723–1730.

Greider,C.W. (1996) Telomere length regulation. *Annu. Rev. Biochem*., **65**, 337–365.

Greider,C.W. and Blackburn,E.H. (1989) A telomeric sequence in the RNA of *Tetrahymena* telomerase required for telomere repeat synthesis. *Nature*, **337**, 331–337.

Hande,P., Slijepcevic,P., Silver,A., Bouffler,S., Van Buul,P., Bryant,P. and Lansdorp,P. (1999a) Elongated telomeres in Scid mice. *Genomics*, in press.

Hande,P., Samper,E., Lansdorp,P. and Blasco,M.A. (1999b) Telomere length dynamics and chromosomal instability in cells derived from telomerase null mice. *J. Cell Biol*., in press.

Hanish,J.P., Yanowitz,J.L. and de Lange,T. (1995) Stringent sequence requirements for the formation of human telomeres. *Proc. Natl Acad. Sci. USA*, **91**, 8861–8865.

Harrington,L., Zhou,W., McPhail, T, Oulton,R., Yeung,D., Mar,V., Bass,M.B. and Robinson,W. (1997a) Human telomerase contains evolutionarily conserved catalytic and structural subunits. *Genes Dev*., **11**, 3109–3115.

Harrington,L., McPhail,T., Mar,V., Zhou,W., Oulton,R., Bass,M.B., Arruda,I. and Robinson,M.O. (1997b) A mammalian telomerase-associated protein. *Science*, **275**, 973–977.

Harris,M.J. and Juriloff,D.M. (1997) Genetic landmarks for defects in mouse neural tube closure. *Teratology*, **56**, 177–187.

Imamoto,A. and Soriano,P. (1993) Disruption of the *csk* gene, encoding a negative regulator of src family tyrosine kinases, leads to neural tube defects and embryonic lethality in mice. *Cell*, **73**, 1117–1124.

Kilian,A., Bowtell,D.D.L., Abud,H.E., Hime,G.R., Venter,D.J., Keese,P.K., Duncan,E.L., Reddel,R.R. and Jefferson,R.A. (1997) Isolation of a candidate human telomerase catalytic subunit gene, which reveals complex splicing patterns in different cell types. *Hum. Mol. Genet.*, **6**, 2011–2019.

Kiyono,T., Foster,S.A., Koop,J.I., McDougall,J.K., Galloway,D.A. and Klingelhutz,A.J. (1998) Both Rb/p16^{INK4a} inactivation and telomerase activity are required to immortalize human epithelial cells. *Nature*, **396**, 84–88.

Lee,H.-W., Blasco,M.A., Gottlieb,G.J., Horner,J.W., Greider,C.W. and DePinho,R.A. (1997) Essential role of mouse telomerase in highly proliferative organs. *Nature*, **392**, 569–574.

Lingner,J., Hughes,T.R., Schevchenko,A., Mann,M., Lundblad,V. and Cech,T. (1997) Reverse transcriptase motifs in the catalytic subunit of telomerase. *Science*, **276**, 561–567.

Martens,U.M., Zijlmans,J.M., Poon,S., Dragowska,W., Yui,J., Chavez,E., Ward,R. and Lansdorp,P.M. (1998) Short telomeres on human chromosome 17p. *Nature Genet.*, **18**, 76–80.

Martín-Rivera,L., Herrera,E., Albar,J.P. and Blasco,M.A. (1998) Expression of mouse telomerase catalytic subunit in embryos and adult tissues. *Proc. Natl Acad. Sci. USA*, **95**, 10471–10476.

McEachern,M.J. and Blackburn,E.H. (1995) Runaway telomere elongation caused by telomerase RNA gene mutations. *Nature*, **376**, 403–409.

Meyerson,M. *et al*. (1997) hEST2, the putative human telomerase catalytic subunit gene, is upregulated in tumor cells and during immortalization. *Cell*, **90**, 785–795.

Naito,T., Matsuura,A. and Ishikawa,F. (1998) Circular chromosome formation in a fission yeast mutant defective in two ATM homologues. *Nature Genet.*, **20**, 203–206.

Nakamura,T.M., Morin,G.B., Chapman,K.B., Weinrich,S.L., Andrews,W.H., Lingner,J., Harley,C.B. and Cech,T. (1997) Telomerase catalytic subunit homologs from fission yeast and human. *Science*, **277**, 955–959.

Nakamura,T.M., Cooper,J.P. and Cech,T. (1998) Two modes of survival of fission yeast without telomerase. *Science*, **282**, 493–496.

Nakayama,J., Saito,M., Nakamura,H., Matsuura,A. and Ishikawa,F. (1997) *TLP1*: a gene encoding a protein component of mammalian telomerase is a novel member of WD repeat family. *Cell*, **88**, 875–884.

Niida,H., Matsumoto,T., Satoh,H., Shiwa,M., Tokutake,Y., Furuici,Y. and Shinkai,Y. (1998) Severe growth defect in mouse cells lacking the telomerase RNA component. *Nature Genet.*, **19**, 203–206.

Nugent,C.I. and Lundblad,V. (1998) The telomerase reverse transcriptase: components and regulation, *Genes Dev.*, **12**, 1073–1085.

Putz,B. and Morriss-Kay,G. (1981) Abnormal neural fold development in trisomy 12 and trisomy 14 mouse embryos. *J. Embryol. Exp. Morphol.*, **66**, 141–158.

Sah,V.P., Attardi,L.D., Mulligan,G.J., Williams,B.O., Bronson,R.T. and Jacks,T. (1995) A subset of p53-deficient embryos exhibit exencephaly. *Nature Genet.*, **10**, 175–180.

Sakai,Y. (1989) Neurulation in the mouse: manner and timing of neural tube closure. *Anat. Rec.*, **223**, 194–203.

Sandell,L.L. and Zakian,V.A. (1993) Loss of a yeast telomere: arrest, recovery and chromosome loss. *Cell*, **75**, 729–739.

Shay,J.W. and Bacchetti,S. (1997) A survey of telomerase activity in human cancer. *Eur. J. Cancer*, **33**, 787–791.

Singer,M.S. and Gottschling,D.E. (1994) TLC1: template RNA component of the *Saccharomyces cerevisiae* telomerase. *Science*, **266**, 387–388.

Tassabehji,M., Read,A.P., Newton,V.E., Harris,R., Balling,R., Gruss,P. and Strachan,T. (1992) Waardenburg's syndrome patients have mutations in the human homologue of the Pax-3 paired box gene. *Nature*, **355**, 635–636.

Wang,J., Xie,L.Y., Allan,S., Beach,D. and Hannon,G.J. (1998) Myc activates telomerase. *Genes Dev.*, **12**, 1769–1774.

Wright,W.E., Piatyszek,M.A., Rainey,W.E., Bryd,W. and Shay,J.W. (1996) Telomerase activity in human germline and embryonic tissues and cells. *Dev. Genet.*, **18**, 173–179.

Yashima,K., Maitra,A., Timmons,C.F., Rogers,B.B., Pinar,H., Milchgrub,S., Wright,W.E., Shay,J.W. and Gazdar,A.F. (1998) Expression of the RNA component of human telomerase during development and differentiation. *Cell Growth Differ.*, **9**, 805–813.

Zijlmans,J.M., Martens,U.M., Poon,S., Raap,A.K., Tanke,H.J., Ward,R.K. and Lansdorp,P.M. (1997) Telomeres in the mouse have large inter-chromosomal variations in the number of T2AG3 repeats. *Proc. Natl Acad. Sci. USA*, **94**, 7423–7428.

Received September 11, 1998; revised November 17, 1998; accepted January 1, 1999